Journal of Molecular Liquids 382 (2023) 121893

Contents lists available at ScienceDirect

Journal of Molecular Liquids

journal homepage: www.elsevier.com/locate/molliq

Bioactive *trans*-resveratrol as dispersant of graphene in water. Molecular interactions

Carlos Sainz-Urruela [a], Soledad Vera-López [a,b], Ana M. Díez-Pascual [a,b], María Paz San Andrés [a,b,*]

[a] Universidad de Alcalá, Facultad de Ciencias, Departamento de Química Analítica, Química Física e Ingeniería Química, Ctra. Madrid-Barcelona Km. 33.6, 28805 Alcalá de Henares, Madrid, Spain

[b] Universidad de Alcalá, Instituto de Investigación Química Andrés M. del Río (IQAR), Ctra. Madrid-Barcelona Km. 33.6, 28805 Alcalá de Henares, Madrid, Spain

ARTICLE INFO

Keywords:
Resveratrol
Graphene
Dispersion
Fluorescence

ABSTRACT

Currently, the preparation of high-quality graphene (G) dispersions is crucial due to the increasing demand for this nanomaterial in a wide range of industries. However, given the strong π–π stacking tendency between G sheets, dispersant agents such as surfactants or polymers are required to attain stable and homogenous dispersions in liquid media. In the present work, the effectiveness of resveratrol (RV), a fluorescent bioactive compound with antioxidant activity, as a dispersing agent for G in aqueous solutions was assessed. The interaction between G and RV was investigated via absorbance, fluorescence and Raman measurements. Dispersions were prepared via bath sonication, followed by probe ultrasonication and centrifugation, though the two last stages have little effect on the dispersion quality. The addition of G causes a quenching on RV fluorescence, and its magnitude raises with increasing G concentration, being the effect stronger up to 10 mg L^{-1}. The change in the centrifugation speed and time have hardly influence on the RV fluorescence in the presence of G. The RV content remaining in the bulk solution after G dispersion, measured via UV–Vis absorption, decreases linearly with increasing G concentration. RV can effectively disperse all the G present in the sample up to 10 mg L^{-1}; at higher concentrations, the dispersing ability slightly decreases, and the G content is distributed between the bulk solution and the centrifuged residue. Besides, the fluorescence of RV dispersed in G is much higher in methanol than in an aqueous medium. TEM analysis confirms the good exfoliation of G upon ultrasonication in RV solutions and indicates that the layer thickness depends on the G/RV ratio. The results of this study could open new perspectives for using natural products like resveratrol as biocompatible and efficient dispersing agents of G to be used in numerous applications, especially in biomedicine.

1. Introduction

Resveratrol (3,4′,5 trihydroxystilbene) is a natural polyphenol that has been found in a large number of plant species, particularly in grapes skin, blueberries, raspberries, mulberries and peanuts, and also occurs in red wines and several human foods [1]. It is a stilbenoid with two phenol rings linked to each other by an ethylene bridge, and a phytoalexin that acts against pathogens, including bacteria and fungi. It exists in cis- and trans- isomeric forms (Fig. 1), however, it is the trans- form which is extracted from plants and has biological activity. The *cis*-isomer has never been identified in grape extract, although it is possible to get it, by irradiating the *trans*-isomer with UV light [2].

Many works have confirmed the very high antioxidant activity of *trans*-resveratrol [3,4]. It also displays antitumor activity, and it is regarded as a promising candidate for cancer prevention and treatment. In fact, numerous *in vitro* and *in vivo* studies have corroborated its anticancer properties and demonstrated that this compound has the ability to hinder all carcinogenesis steps. Furthermore, other bioactive effects including cardioprotective, vasorelaxant, anti-inflammatory, phytoestrogenic and neuroprotective have been described [5–8]. Even so, due to its poor solubility in water and bioavailability, resveratrol use is still a main dare for the pharmaceutical industry. Despite it is present in diverse vegetables and fruits, it is found in higher concentration in grapes, followed by red wine, in which *trans*-resveratrol content ranges

* Corresponding author at: Universidad de Alcalá, Facultad de Ciencias, Departamento de Química Analítica, Química Física e Ingeniería Química, Ctra. Madrid-Barcelona Km. 33.6, 28805 Alcalá de Henares, Madrid, Spain.
E-mail address: mpaz.sanandres@uah.es (M.P. San Andrés).

https://doi.org/10.1016/j.molliq.2023.121893
Received 18 November 2022; Received in revised form 12 April 2023; Accepted 19 April 2023
Available online 24 April 2023
0167-7322/© 2023 The Author(s). Published by Elsevier B.V. This is an open access article under the CC BY-NC-ND license (http://creativecommons.org/licenses/by-nc-nd/4.0/).

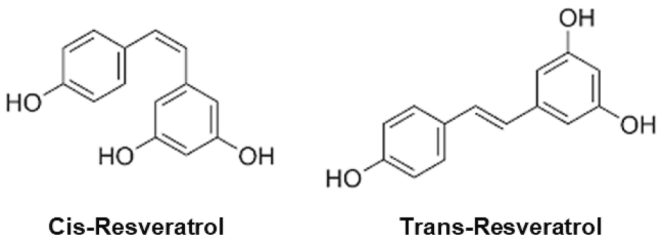

Fig. 1. Chemical structure of the trans- and cis- isomers of resveratrol.

between 0.1 and 15 mg L^{-1} depending on the growing country [2]. It is hardly soluble in water (solubility lower than 1 mg mL^{-1}), but it has good solubility in ethanol, dimethyl sulfoxide and other organic solvents.

The biological activity of resveratrol depends on the pH of the medium. Its three acidic dissociation constants in aqueous medium are $pK_{a1} = 8.8$, $pK_{a2} = 9.8$, and $pK_{a3} = 11.4$ [9]. Trans-resveratrol is a fluorescent compound, with a maximum emission peak at 385 nm. Its fluorescence is dependent on the concentration and the pH, being stronger in acid and neutral media, but a drastic decay occurs at pH values higher than 7.0, and a negligible signal is obtained at pH 11.0 and above [10]. Furthermore, it is affected by the viscosity of the medium, being more intense as the viscosity increases. Also, it presents higher solubility in an alcohol medium than in an aqueous solution [11], hence its fluorescence emission in alcohol is more intense. Owing to the important physiological role and the implication of *trans*-resveratrol level, numerous analytical techniques have been reported for its quantification [12]. The detection via chromatographic and electrophoretic methods has high sensitivity and specificity, although these methods are time-consuming. Fluorescence spectroscopy is a suitable technique to determine the interaction between resveratrol and biological compounds such as proteins (ie. serum albumins [13]). Many models based on the fluorescence quenching of proteins by *trans*-resveratrol have been used such as the Stern–Volmer equation, double logarithm regression curve, Lineweaver–Burk curve, Levine equation and Tachiya model [14]. However, the obtained binding constants were different when considering the different models or equations.

Amongst carbon nanomaterials, graphene, a single monolayer of graphite, has attracted a lot of attention due to its unique properties such as very high thermal and electrical conductivity, superior elasticity combined with flexibility, very high electron mobility, high hardness and stiffness and optical transparency [15]. However, graphene is hydrophobic in nature and tends to aggregate via van der Waals forces among adjacent sheets, which strongly limits its practical applications. Thus, the magnitude of property improvement is, to a large extent, dependent upon the state of dispersion of graphene sheets in a medium [16]. Only when graphene sheets are homogeneously dispersed, the enhancement could be more significant. Different strategies have been described to produce homogeneous and stable G dispersions in liquid media, such as the use of surfactants of different nature and charge [17,18], as well as the covalent and non-covalent functionalization with polymers [19]. Recently, the use of bioactive compounds to attain stable dispersions of graphene and its derivatives in water has been reported [20]. Further, these compounds can simultaneously act as reducing, capping and functionalizing agents, enabling the preparation of eco-friendly nanomaterials in a single step. In particular, tannic acid, a water-soluble polyphenolic compound that comprises many hydroxyl groups, similar to resveratrol, has been found to be an efficient environmentally friendly dispersing agent for graphene and graphene oxide [21,22]. Recently, a flavonoid compound, catechin, with redox properties, has been used to produce graphene via sonochemical exfoliation of graphite in water [23,24]. In addition, a polyphenol solution obtained from a Eucalyptus bark extract has been used to reduce exfoliated GO to soluble graphene under reflux conditions in an aqueous medium [25]. These studies make evident the high potential of bioactive compounds to yield stable dispersions of graphene via sonication in an aqueous medium as a simple, cheap and sustainable medium.

In the aforementioned studies, the bioactive compound used as a dispersant agent was not fluorescent, hence, to assess its dispersant capability, a fluorescent biomolecule such as riboflavin acting as a fluorescent probe was necessary [21,22]. Both graphene and graphene oxide dispersed in tannic acid were found to cause a quenching effect on riboflavin fluorescence, which depended on many factors such as the concentration of the carbon nanomaterial and the dispersant, their weight ratio, the pH of the medium and the use of a centrifugation stage for the preparation of the dispersions.

In the present study, the efficiency of *trans*-resveratrol (RV) as a dispersing agent for graphene has been evaluated for the first time. Since this polyphenol is fluorescent, its dispersant efficiency can be directly assessed via fluorescence spectroscopy. The fluorescence of resveratrol is quenched in the presence of graphene due to strong interactions between both compounds. Thus, it has been reported that this polyphenol strongly interacts with graphene-related materials via π-π stacking [26]. Besides, the concentration of resveratrol remaining in the bulk solution after the graphene dispersion has been measured via UV–Vis absorption spectroscopy [27], taking into account the reported absorption coefficient for graphene at 660 nm [28]. It has also been found that the fluorescence of resveratrol dispersed in graphene is much higher in methanol than in an aqueous medium, and this this could be used to recover resveratrol from natural products such as wine.

2. Materials and methods

2.1. Materials and reagents

Graphene, made up of less than six sheets with an average thickness of ≤ 2 nm, oxygen content (XPS): 5%, was supplied by Avanzare Innovación Tecnológica SL. (Logroño, Spain). Powdered resveratrol (3,5,4′-trihydroxy-*trans*-stilbene, $C_{14}H_{12}O_3$, $M_w = 228.24$ g/mol, ≥99% HPLC), was obtained from Sigma-Aldrich (Madrid, Spain) and used as received. Methanol ($M_w = 32.04$ g/mol, $d_{25°C} = 0.791$ g/cm^3) was acquired from Scharlab (Barcelona, Spain). Ultrapure water was purified by a Millipore system (Millipore, Milford, CT, USA).

2.2. Instrumentation

An FL6500 fluorescence spectrometer from PerkinElmer (Waltham, MA, USA) was used to register the fluorescence spectra at 25 ± 1 °C with a Digiterm S-150 bath from Selecta (Barcelona, Spain). The excitation and emission slits were set at 5 nm and the scan speed was 500 nm min^{-1}. Quartz cuvettes with a 1 cm path length were used for the measurements. The acquisition and data analysis were carried out using the Perkin-Elmer Flwin Lab software.

A Lambda 35 UV–Vis spectrometer from PerkinElmer (Waltham, MA, USA) was used to measure the absorbance of the resveratrol dispersions in graphene, with a slit width of 1 nm and a scan speed of 480 nm min^{-1}.

Resveratrol dispersions were prepared with an Elmasonic S40 ultrasound bath (Elma Schmidbauer GmbH, Singen, Germany) at a frequency of 37 kHz, a Hielscher UP400S ultrasound probe (Teltow, Germany) with a sonotrode of 3 mm diameter and 100 mm lenght working at 400 W and 40% amplitude (160 W, 9.6 kHz), and an Orto Alresa Digicen centrifuge (Madrid, Spain).

A Zeiss EM-10C/CR transmission electron microscope (Oberkochen, Germany) operating at 60 kV was used to assess the quality of the graphene dispersions in resveratrol.

Raman spectra were acquired using a high performance in Via confocal Raman instrument (Renishaw, Gloucestershire, UK) equipped with a Nd:YAG 532 nm laser. Five scans were recorded for each sample at a power of 500 mW.

2.3. Preparation of graphene dispersions

Graphene dispersions were prepared at room temperature, at concentrations ranging from 0 to 80 mg L^{-1}. The G amount needed for each dispersion was weighed in a centrifuge tube, and 50 mL of a RV solution with the appropriate concentration (in the range between 0 and 10 mg L^{-1}) was added to the tube. RV stock solution 1.6 g L^{-1} was prepared in methanol, and the required milliliters were taken and diluted with ultrapure water. Subsequently, each dispersion was sonicated in a US bath at a frequency of 37 kHz for 30 min followed by 5 min of continuous ultrasonication with a 3 mm diameter probe at 160 W (9.6 kHz). During probe sonication, dispersions were immersed in an ice-water bath to prevent from overheating. Then, they were centrifuged for 15 min at 4000 rpm to remove the undesirable large particles that were not dispersed.

2.4. Fluorescence spectra

Fluorescence contour graphs were recorded in water and methanol at a concentration of 2.5 mg L^{-1} and the measured pH was 5.8. The initial excitation wavelength was set at 220 nm, and 10 spectra were registered with an increment of 10 nm. The fluorescence emission spectra of RV were recorded at the maximum excitation wavelength, that is, 320 nm in water and 300 nm in methanol.

2.5. Absorption spectra

Absorption spectra were recorded in water for RV concentrations of 2.5 and 5.0 mg L^{-1} and G concentrations ranging between 0 and 40 mg L^{-1}. These measurements were carried out using dispersions obtained after sonication and centrifugation.

2.6. Desorption of resveratrol

After the preparation of 50 mL of the dispersions, a certain amount of RV remains absorbed on the solid G sheets at the bottom of the tube that is removed during the process. To determine the concentration of RV adsorbed onto G, and to recover this compound, the supernatant was separated, 50 mL of methanol were added and the mixture was centrifugated. The amount of RV in the methanol solution was quantified by fluorescence after centrifugation of the mixture. In some dispersions with 20 mg L^{-1} of G, a lower volume of methanol (ie. 25 mL and 10 mL) was added to concentrate the RV.

3. Results and discussion

3.1. Fluorescence spectra of resveratrol

The fluorescence spectra of resveratrol were registered as 3D contour graphs. Fig. 2 shows the spectra of RV 2.5 mg L^{-1} in water and MeOH.

As can be observed in Fig. 2, the spectrum of RV appears at a higher excitation wavelength in water (320 nm) than in MeOH (300 nm). With regard to the emission wavelength, the value is similar for both media: in water appears at 396–407 nm and in MeOH at 391 nm. The fluorescence intensity is higher in MeOH, being a value about double that in water. This is due to the higher solubility of RV in the polar organic solvent than in water [11].

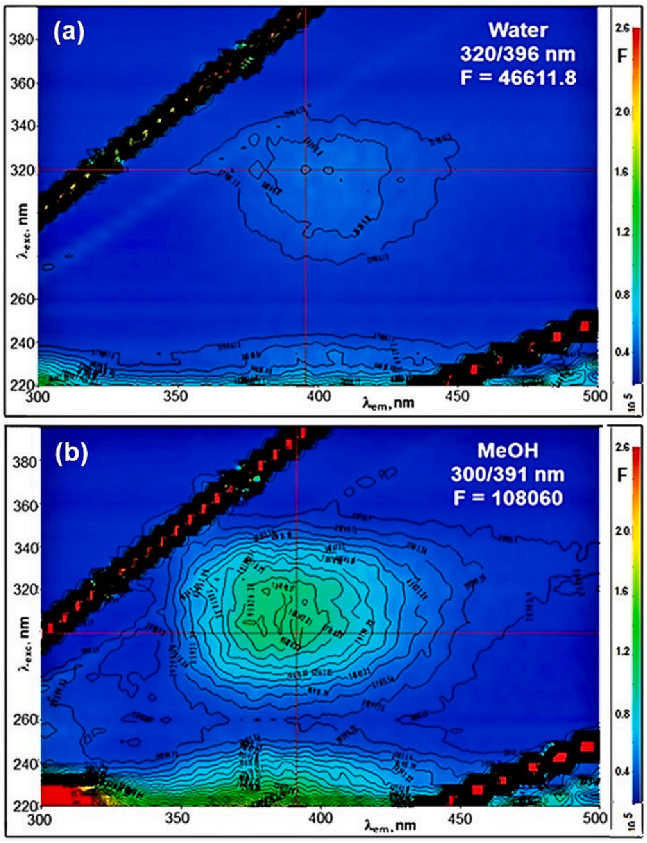

Fig. 2. Fluorescence contour graphs of RV 0.4 mg L^{-1} in (a) water and (b) MeOH.

3.2. Study of resveratrol stability in water

Prior to carrying out the dispersion process of G in resveratrol, during which the active compound could be degraded, it is important to check its stability under the dispersion experimental conditions. As described in the experimental section, for the preparation of the G dispersions, the solution is first sonicated in an ultrasonic bath, followed by sonication with a high-power ultrasonic probe and then centrifugation. To test the stability, a RV aqueous solution (2.5 mg L^{-1}) was subjected to sonication in the bath for 30 min and in the sonication probe for another 30 min. As can be observed in Fig. 3, none of the two sonication types induced a significant effect on the fluorescence intensity of RV. These results indicate that neither the sonication with the bath nor with the bath and probe damage the RV molecule. The centrifugation effect on the fluorescence intensity of RV was also tested, and a slight decline in the intensity was observed (Fig. 3).

As can be observed in Fig. 3, the decrease in the fluorescence intensity for the centrifuged sample compared with the RV one is just 5.5%, which is not very significant.

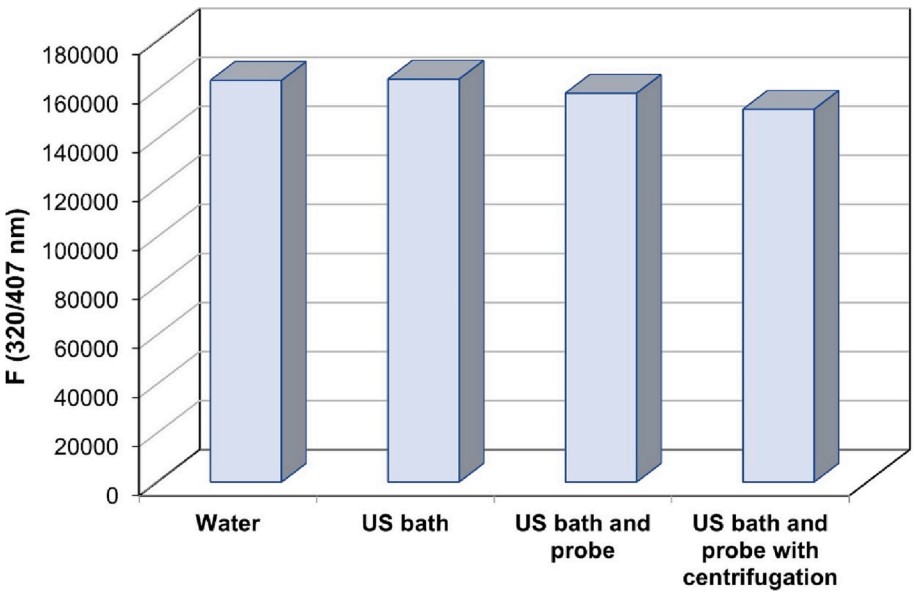

Fig. 3. Fluorescence intensity of RV 2.5 mg L^{-1} in water and after ultrasonication in bath, ultrasonication in bath and ultrasonic probe and after ultrasonication with bath and probe and centrifugation.

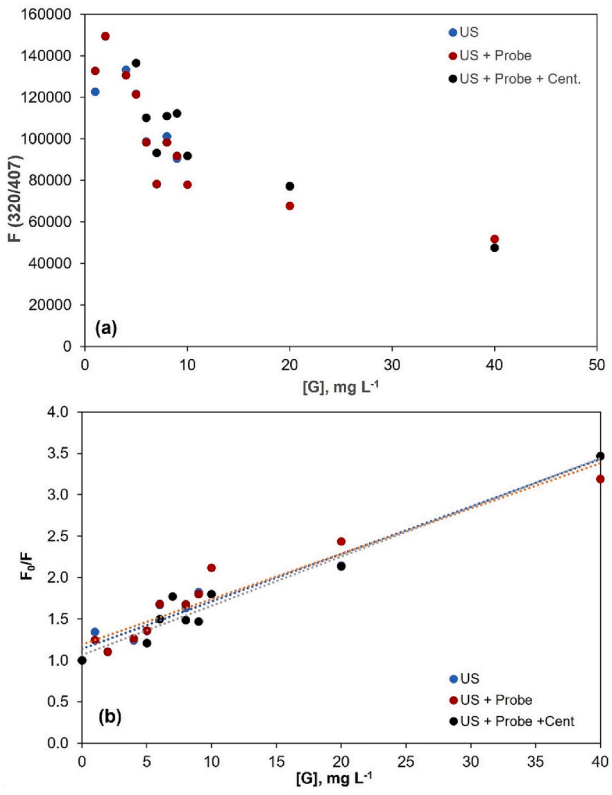

Fig. 4. (a) Fluorescence intensity and **(b)** Stern-Volmer plot of RV 2.5 mg L^{-1} solution in water in the presence of G concentrations ranging from 0 to 40 mg L^{-1}, without and with 30 min ultrasonic bath, 5 min ultrasonic probe at 160 W and centrifugation for 15 min at 4000 rpm.

3.3. Graphene dispersions in resveratrol

3.3.1. Fluorescence measurements

Once it was probed that the RV structure does not suffer degradation after sonication nor centrifugation, graphene was dispersed using resveratrol as the dispersant. To study the interaction between G and RV and the resulting dispersions, absorbance and fluorescence were measured. Fig. 4**a** shows the fluorescence measurements of RV 2.5 mg L^{-1} solution in water in the presence of G concentrations ranging from 0 to 40 mg L^{-1}, prepared using ultrasounds in a bath for 30 min, an ultrasonic probe for 5 min at 160 W and a centrifugation stage for 15 min at 4000 rpm.

All the solutions were subjected to sonication in an ultrasonic bath, an ultrasonic probe and after that, to centrifugation. The decrease in the fluorescence of resveratrol indicates an interaction with G that produces a quenching effect over the resveratrol fluorescence.

The results clearly show the decrease in the fluorescence as graphene concentration is increased up to 10 mg L^{-1}, while for higher concentrations the fluorescence of RV decreases with a lower slope. The values obtained using US bath, US probe and centrifugation are similar and thus, it can be concluded that the US power and centrifugation have no effect on the dispersion. Fig. 4**b** shows the Stern-Volmer relationship with a good correlation for the three cases. A clear decrease in fluorescence intensity is observed when graphene is added. The higher the graphene concentration, the lower the intensity of RV fluorescence, which suggests that RV only emits fluorescence when it is free in the bulk solution and not on the G surface. The quenching effect exerted by graphene is likely due to the binding between both molecules. This fact indicates that the maximum dispersion is achieved with the ultrasonic bath, and that RV is not affected as more stages are added.

Table 1 shows the calculated intercept, slope and R^2 for the three cases. The quenching constants correspond to the slope of the different curves.

Table 1
Regression parameters of the Stern-Volmer plot using an ultrasonic bath, ultrasonic bath and probe, and ultrasonic bath, probe and centrifugation.

	US Bath	US Bath + Probe	US Bath + Probe + Centrifugation
Intercept	1.07 ± 0.07	1.06 ± 0.06	1.08 ± 0.09
K, L mg^{-1}	0.061 ± 0.008	0.054 ± 0.004	0.058 ± 0.005
R^2, %	91.1	95.3	95.3

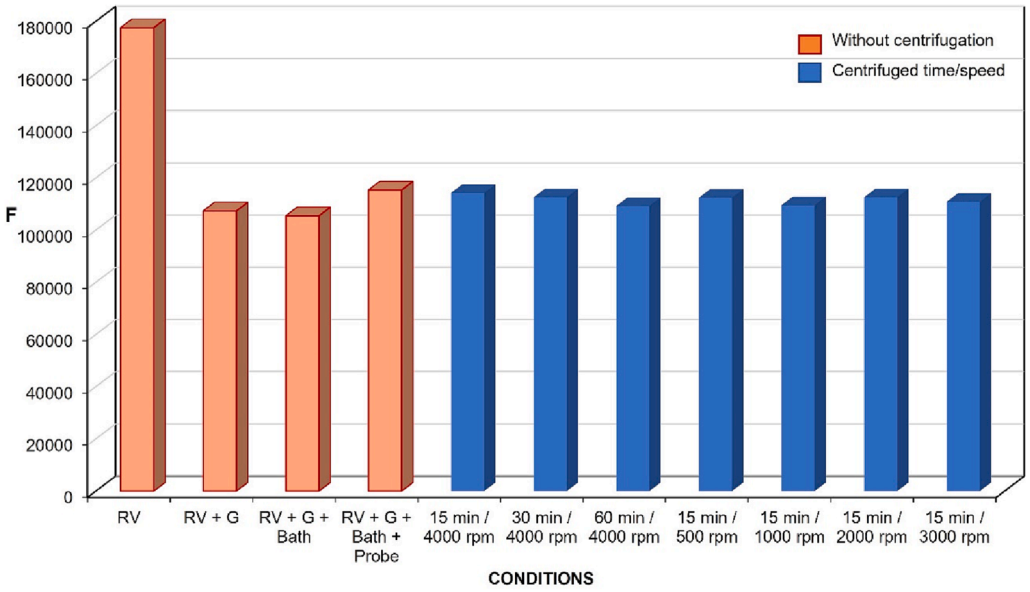

Fig. 5. Fluorescence intensity of RV 2.5 mg L^{-1} and RV 2.5 mg L^{-1} + G 20 mg L^{-1} without and with ultrasonic bath, ultrasonic probe and different centrifugation conditions.

As can be observed in Table 1, the intercept of the curves in the three cases are 1 considering the error, and the quenching constants are very similar. Therefore, the use of the ultrasonic probe and centrifugation have hardly any effect on the interaction of RV with G.

Besides, the influence of different experimental conditions during the centrifugation step on the fluorescence intensity of RV in presence of G 20 mg L^{-1} was assessed. The parameters investigated were centrifugation time and speed, which ranged from 5 to 60 min and 500 to 4000 rpm, respectively. Fig. 5 shows the fluorescence intensity values obtained for RV in water, in the presence of G with bath and probe (red bars) and for the different conditions during the centrifugation step (blue bars).

The change in centrifugation speed and time did not modify the fluorescence of RV, which interacts with G even in the absence of additional energy. This fact indicates that the interaction of RV with G takes place when both molecules are in contact, even if the G dispersion is not very good, since in the absence of ultrasonic energy, G is aggregated in the bulk solution, although it interacts with RV. The visual difference between the centrifugated and non-centrifugated solutions can be observed in **Figure S1** for G 0.5 and 5 mg L^{-1} dispersions, which compares the photographs of both types of samples.

3.3.2. *Absorption spectrophotometry measurements*

Additionally, the absorbance of G dispersions in RV has been measured at two wavelengths, 660 nm and 354 nm. At 660 nm, the absorbance value corresponds to the light dispersion caused by the G flakes dispersed in the solution. At this wavelength, RV molecules do not absorb radiation. On the other hand, RV absorbance in water shows a maximum at 354 nm, which has been used for measuring the RV concentration that remains in the bulk solution after G dispersion. Fig. 6 shows the decrease found in the absorbance of RV as the G concentration increases, at 354 and 660 nm.

The RV concentration in the bulk solution decreases linearly at 354 nm, due to the interaction that occurs between G and RV, which is adsorbed onto its surface (Fig. 6**a**). For an initial RV concentration of 2.5 mg L^{-1}, the value of the absorbance in the presence of 40 mg L^{-1} G is almost zero, which indicates that in the bulk solution there is only a small amount of RV, and it is absorbed on the G surface. As can be observed in Table 2**,** the RV concentration decreases with increasing the amount of G.. Therefore, the RV concentration adsorbed on the G sheets is the difference between these values and the RV initial concentration These initial values are plotted in the linear calibration curve shown in **Figure S2**.

Regarding the absorbance at 660 nm, it reaches a maximum when graphene is added that is the maximum amount of G that can be dispersed for each RV concentration. Thus, as can be observed in Fig. 6**b**, the absorbance raises with increasing G concentration up to a maximum at approximately 10 mg L^{-1} while it decreases for higher G concentrations when the RV concentration is 2.5 mg L^{-1}. However, for a RV concentration of 5 mg L^{-1}, the maximum is reached at about double G concentration (20 mg L^{-1}). Results suggest that the RV role as a dispersant agent for G is effective only up to a maximum concentration that depends on the G/RV ratio. As can be observed in Fig. 6**c**, the absorbance as a function of G/RV ratio reaches a maximum at a similar value (about 4) for both RV concentrations. Therefore, the G amount dispersed by RV depends on the concentrations of both compounds and mainly on the G/RV ratio.

To further study the absorbance of G in the dispersions, the different dispersions were diluted and the absorbance at 660 nm was measured. Fig. 7**a** shows, as an example, the change in the absorbance as a function of G concentration obtained for each dispersion in RV 2.5 mg L^{-1}. As can be observed, a linear trend is found in all cases, and the slope of the curves decreases with increasing G concentration. Fig. 7**b** displays the slopes as a function of G concentration for both RV concentrations, 2.5 and 5.0 mg L^{-1}. In both cases, the slope decreases exponentially with G concentration and remains almost unchanged for concentrations higher than 10 mg L^{-1}. This behavior could be explained considering that at low G concentration, RV can effectively disperse all the G present in the sample; while at higher G concentrations, RV is not able to disperse the whole amount of G, meaning that the G content is distributed between that dispersed in the bulk solution and that centrifuged at the bottom of the tube.

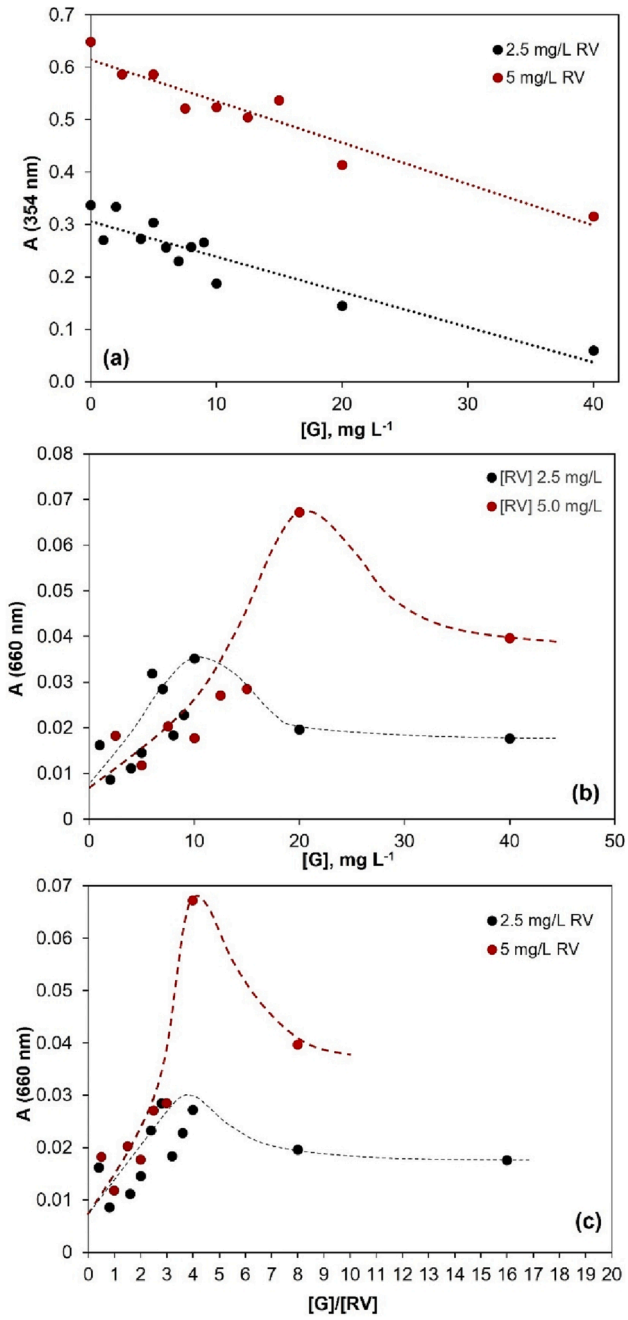

Fig. 6. Absorbance of G dispersions in RV as a function of G concentration at 354 nm (a); absorbance of G dispersions in RV as a function of G concentration at 660 nm (b) and absorbance of G dispersions in RV as a function of [G]/[RV] ratio at 660 nm (c).

Table 2
RV concentration in the bulk solution after G dispersion for increasing G concentrations.

[G] , mg L^{-1}		0	10	20	40
[RV] , mg L^{-1}	$[RV]_S = 5.0$	4.647	3.757	2.974	2.271
	$[RV]_S = 2.5$	2.429	1.362	1.060	0.454

$[RV]_S$: RV concentration in the solution before G dispersion.

3.3.3. *Desorption of resveratrol from graphene sheets*

As mentioned earlier, the RV used as G dispersant is distributed between two different phases. One is the bulk solution, in which remains the RV that has not been adsorbed onto the graphene sheets. Such

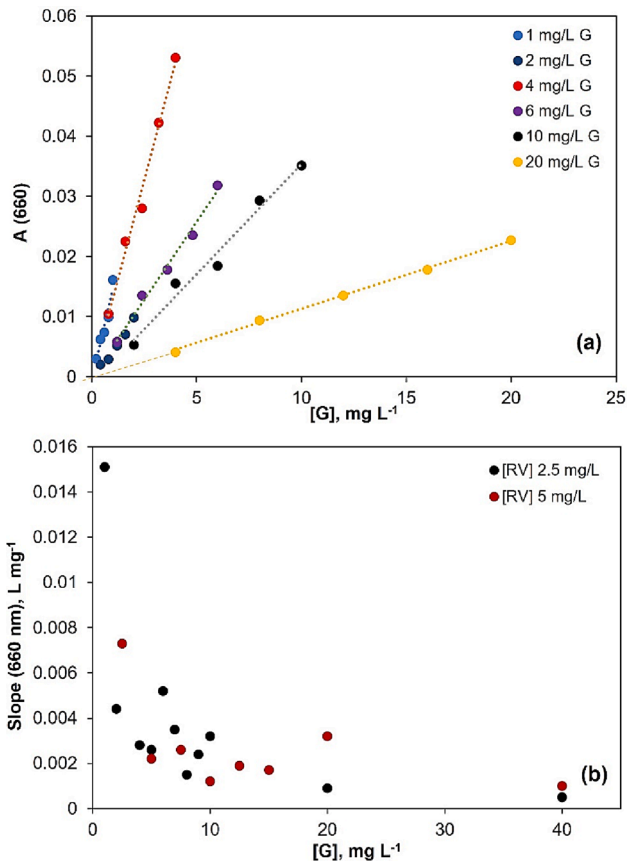

Fig. 7. Absorbance of diluted G dispersions in RV 2.5 mg L^{-1} at 660 nm (a). Slopes of the linear relationship between absorbance and G concentration for the diluted G dispersions in RV 2.5 and 5.0 mg L^{-1} (b).

amount was calculated as indicated in section 3.3.2, and the RV concentrations are given in **table 2**. The another one is the RV adsorbed on the G sheets, and during the centrifugation step it is divided into the G dispersed sheets and the G sheets that settle at the bottom of the tube.

In order to calculate the amount of RV deposited at the bottom of the tube, and thus, removed from the dispersion, it was desorbed using methanol as solvent. RV is slightly soluble in water, but highly soluble in polar organic solvents such as methanol. The removal of the dispersion after centrifugation leads to an agglomerated solid, and by adding the same volume of MeOH as the dispersion volume or lower, this RV adsorbed on the G sheets is solubilized. Fig. 8 shows the linear relationship obtained for RV in MeOH and the fluorescence values obtained in the methanol phase after recovering the RV from the solid residue.

Table 3 shows the RV concentration determined in MeOH extract and the percentages desorbed with respect to the total RV concentration. As it can be observed, the amount of RV desorbed is in most cases around 50% of the initial RV concentration. In addition, by using a smaller volume of MeOH it is possible to concentrate the RV desorbed, although the recovery attained is smaller than that found for 50 mL as can be observed for G 20 and 40 mg L^{-1} using 25 and 10 mL of MeOH for desorption.

The average percentage of RV recovery is 41.3, and there are not significant statistical differences between the values of the two variables, RV initial concentration and G concentration studied by Analysis of Variance (ANOVA) multifactorial for a 95% confidence (P-value = 0.43 for RV concentration and 0.19 for G concentration). **Figure S3** shows the confidence intervals obtained for the RV recovery with methanol 50 mL for each initial RV concentration.

Taking into account the data gathered in Tables 2 and 3, we can estimate the amount of RV that is in the different phases when the

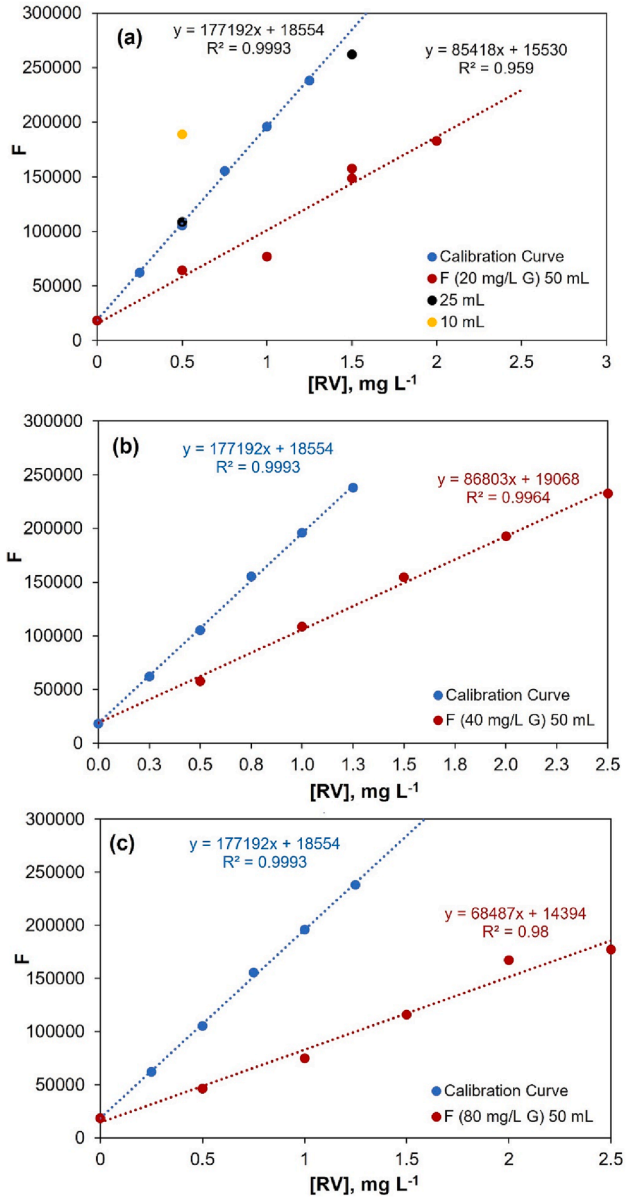

Fig. 8. Fluorescence of the RV recovered from the residue of G dispersions at concentrations of (a) 20 mg L^{-1}, (b) 40 mg L^{-1} and (c) 80 mg L^{-1}.

dispersion is obtained. For an initial RV concentration of 2.5 mg L^{-1} (measured 2.43 mg L^{-1}, see Table 2), the concentration that remains in the bulk solution is 1.06 mg L^{-1}. The RV concentration linked to G is 1.4 mg L^{-1}, which is the sum of the solid deposited at the bottom and that adsorbed on the dispersed sheets. Given that the RV recovered in MeOH that was in the solid at the bottom is 0.81 mg L^{-1}, the amount of RV adsorbed on the G sheets dispersed in the medium is 0.60 mg L^{-1}. Analogously, for a G concentration of 40 mg L^{-1}, the amount of RV measured in the bulk solution was 0.45 mg L^{-1} (Table 2) and the RV concentration linked to G is 1.98 mg L^{-1}. As the RV recovered in MeOH from the solid residue is 1.21 mg L^{-1}, the amount of RV adsorbed on the G sheets dispersed in the medium is 0.77 mg L^{-1}. The comparison of the results for the two G concentrations indicates that the higher the G concentration, the lower the RV amount in the bulk solution, and that the amount of RV in the G sheets and in the solid at the bottom increases about double, as well as the initial G concentration.

3.3.4. Raman

To further corroborate the exfoliation of G induced in the presence of

Table 3
Percentage of RV desorbed from the undispersed graphene (centrifugation residue) with MeOH.

$[RV]_0$, mg L^{-1}	[G], mg L^{-1}	V_{MeOH}, mL	$[RV]_F$, mg L^{-1}	% [RV] desorbed
0.5	20	10	0.96	38.5
0.5	20	25	0.51	50.8
0.5	20	50	0.26	51.5
0.5	40	10	0.50	20.1
0.5	40	25	0.38	37.8
0.5	40	50	0.22	44.3
0.5	80	50	0.16	31.3
1.0	20	50	0.33	33.0
1.0	40	50	0.51	50.8
1.0	80	50	0.32	31.8
1.5	20	25	1.38	45.8
1.5	20	50	0.73	48.9
1.5	20	50	0.78	52.3
1.5	40	50	0.77	51.2
1.5	80	50	0.55	36.7
2.0	20	50	0.93	46.3
2.0	40	50	0.98	49.2
2.0	80	50	0.84	42.0
2.5	20	50	0.81	32.4
2.5	40	50	1.21	48.3
2.5	80	50	0.89	35.8

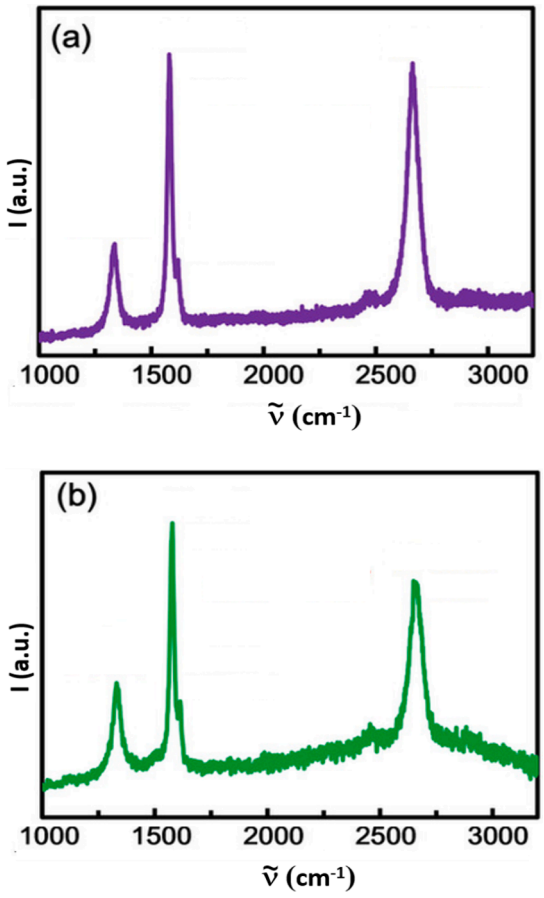

Fig. 9. Raman spectrum of G (a) and G dispersion (20 mg L^{-1}) in RV 2.5 mg L^{-1}.

RV, the Raman spectrum of pristine G and the dispersion with the most effective RV concentration (2.5 mg L^{-1}) were compared. The spectrum of raw G (Fig. 9a) shows four main bands: [29] the G band at 1580 cm^{-1} associated to ordered in-plane vibrations of sp^2 carbon atoms, a small shoulder (Ḍ band) at around 1620 cm^{-1}, ascribed to the disorder of edge carbons, the D band at 1340 cm^{-1} associated with defects and deviations

from perfect order in the sp^2 graphite lattice and the 2D band at 2660 cm^{-1} that originates from a two-phonon double resonance [30].

In the spectrum of G dispersion (20 mg L^{-1}) in RV 2.5 mg L^{-1}, Fig. 9**b, a** change in the position of the bands can be observed. A clear upshift in the 2D band is found (by about 10 cm^{-1}) combined with a widening and reduction in intensity. Taken into account that the shape and position of the 2D band is strongly dependent on the number of G layers [31], this shift is indicative of an increase in the number of graphene layers, likely due to the RV that acts as an exfoliating agent, in agreement with TEM images. The 2D band in monolayer and few layer graphene has been reported to be much more intense and shaper that in multilayer graphene [32]. On the other hand, a small downshift of the G band is found, by about 4 cm^{-1}, which has also been ascribed to an increase in the number of G layers [32].

On the other hand, the intensity of the D band is directly related to the concentration of defects of the graphene layers and depends on the defect type (ie. vacancies, interstitial impurities, sp^3 hybridization). The I_D/I_G ratio is a measure of the disorder degree and is inversely proportional to the average size of the sp^2 domains. Thus, it is used to estimate the amount of defects in graphitic materials: the higher this ratio, the higher the number of defects. The measured I_D/I_G ratio are 0.55 and 0.69, respectively. This increase suggests that RV introduces new defects during the exfoliation process and thus causes a partial disorder at the carbon edges. Further, RV can interact with G via π-π stacking interactions, as well as by hydrogen bonding between the polar hydroxyl groups located at defect sites within the graphene basal plane and acid groups located at the borders with the hydroxyl groups of RV. The adsorption of RV onto G could result in a non-covalent functionalization, hence increased number of defects, as reported earlier upon adsorption of other aromatic molecules [33].

3.3.5. *Morphology of G dispersions in resveratrol*

In order to assess the potential of RV as dispersant agent for graphene, the morphology of G dispersions in RV have been analyzed by

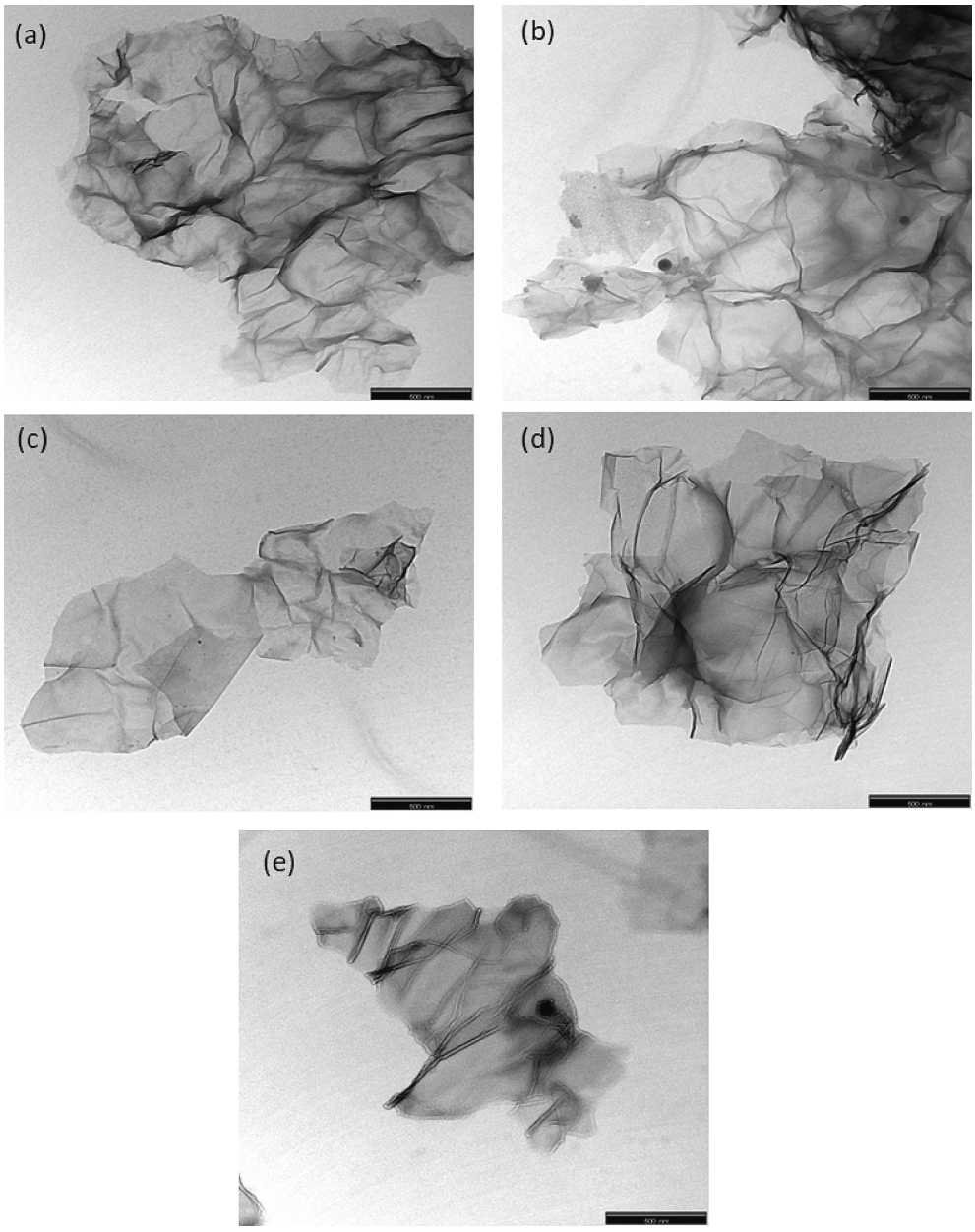

Fig. 10. TEM images for centrifuged samples of graphene (40 mg L^{-1}) dispersions in increasing concentrations of RV: 0.5, 1.0, 1.5, 2.0 and 2.5 mg L^{-1}, respectively, from a) to e) images.

TEM, and representative images obtained for G (40 mg L^{-1}) in different concentrations of RV are compared in Fig. 10. At low RV contents (Fig. 10**a**), the G sheets appear highly wrinkled, with pronounced out-of-plane deformations (ripples), as reported previously for pristine dried G sheets [34]. The sheets are very thin and display a fluffy aspect.

Further, the images reveal the presence of numerous big sheets, larger than 5 μm, in the dispersion. However, with increasing RV content, the surface morphology gradually changes, and the sheets become thicker and less wrinkled. Indeed, the interaction between the medium (RV solutions) and graphene can strongly influence wrinkle- and ripple-formation. Thus, G is hydrophobic in nature, and at low RV contents, would tend to form a more curved structure to minimize the interaction with the surrounding medium. However, with increasing RV content, the G sheets appear to be better dispersed and seem to be thicker and flatter. A likely explanation is that the higher the RV concentration, the nanomaterial is more covered by RV, and the thickness increases. In this case, the images reveal fewer sheets smaller than 1 μm (Fig. 10**e**). When the sheets are wrapped by RV, they will be more hydrophilic and wettable by water. Therefore, they could acquire a water lubrication layer, allowing them to slide on each other, thus avoiding compressing each other. Hydrogen bonding between the OH groups of RV and water may also prevent the sheets from sliding, thus reducing the number of wrinkles [35]. Further, small black spherical dots can be observed in the images with higher RV content, which could arise from RV aggregates, as reported previously for RV-functionalized selenium nanoparticles [36]. Indeed, RV forms aggregates above a certain critical concentration, and this concentration depends on the pH of the medium [37]. G layers wrapped in RV could be stabilized against re-aggregation due to interactions between nearby RV-coated flakes, thus producing quenching on the RV fluorescence, as demonstrated by fluorescence measurements.

Overall, TEM analysis confirms the good exfoliation of G upon ultrasonication in RV aqueous solutions and indicate that the thickness of the layers obtained depend on the G/RV ratio. Besides, it is proven that RV is an efficient dispersant agent for G, which is highly interesting as a green replacement for conventional dispersing agents which are typically unsustainable and environmentally damaging.

4. Conclusions

Herein, a simple, quick and environmentally friendly approach to prepare high-quality G dispersions in both aqueous and organic media has been described. This method permits evading potentially toxic and environmentally harmful dispersing agents often used to attain stable and homogenous G dispersions. RV has been found to be a very good dispersant for G in water as demonstrated by UV–vis spectrophotometry, fluorescence and Raman measurements. The presence of G decreases the fluorescence intensity of RV, and the quenching magnitude depends on several factors, including the concentration of both compounds and their weight ratio, whilst it is hardly influenced by experimental parameters such as the centrifugation speed and time. The RV content outstanding in the bulk solution after G dispersion, drops gradually with increasing G concentration. At relatively low G concentrations, RV can successfully disperse the whole G content present in the sample; however, at high concentrations, RV is not able to completely disperse G, and the nanomaterial content is distributed between the bulk solution and the centrifuged residue at the bottom of the tube. Besides, the fluorescence of RV dispersed in G is much higher in methanol than in an aqueous medium. TEM analysis provides a clear evidence for the good exfoliation of G upon ultrasonication in RV solutions. These findings suggest that a powerful natural antioxidant can be highly efficient in causing G exfoliation in liquid media, and can thus serve as a sustainable substitute for conventional synthetic dispersing agents in large-scale manufacture and applications of graphene-based materials.

CRediT authorship contribution statement

Carlos Sainz-Urruela: Experimental, Writing – original draft.**Soledad Vera-López:** Writing – review & editing. **Ana M. Díez-Pascual:** Writing – review & editing. **María Paz San Andrés:** Methodology, Writing – original draft, Supervision.

Declaration of Competing Interest

The authors declare that they have no known competing financial interests or personal relationships that could have appeared to influence the work reported in this paper.

Data availability

Data will be made available on request.

Acknowledgements

The authors wish to thank the Spanish Ministry of Science and Innovation and Universities (MICIU) for funding the work (Project PGC2018-093375-B-I00). Financial support from the Community of Madrid within the framework of the multi-year agreement with the University of Alcalá in the line of action “Stimulus to Excellence for Permanent University Professors”, Ref. EPU-INV/2020/012, is also acknowledged.

Appendix A. Supplementary material

Supplementary data to this article can be found online at https://doi.org/10.1016/j.molliq.2023.121893.

References

[1] B. Salehi, A.P. Mishra, M. Nigam, B. Sener, M. Kilic, M. Sharifi-Rad, P. Fokou, N. Martins, J. Sharifi-Rad, Resveratrol: A Double-Edged Sword in Health Benefits, Biomedicines 6 (3) (2018) 91, https://doi.org/10.3390/biomedicines6030091.
[2] L. Frémont, Biological Effects of Resveratrol, Life Sci. 66 (2000) 663–673, https://doi.org/10.1016/S0024-3205(99)00410-5.
[3] C. Sainz-Urruela, S. Vera-López, M.P. San Andrés, A.M. Díez-Pascual, Graphene-Based Sensors for the Detection of Bioactive Compounds: A Review, Int. J. Mol. Sci. 22 (2021) 3316, https://doi.org/10.3390/ijms22073316.
[4] H. Kalantari, Das Dipak K, Physiological effects of resveratrol, BioFactors 36 (2010) 401–406, https://doi.org/10.1002/biof.100.
[5] E.B. Rimm, A. Klatsky, D. Grobbee, M.J. Stampfer, Review of Moderate Alcohol Consumption and Reduced Risk of Coronary Heart Disease: Is the Effect Due to Beer, Wine, or Spirits, BMJ 312 (1996) 731–736, https://doi.org/10.1136/bmj.312.7033.731.
[6] A.S. St Leger, A.L. Cochrane, F. Moore, Factors Associated with Cardiac Mortality in Developed Countries with Particular Reference to the Consumption of Wine, Lancet 1 (1979) 1017–1020, https://doi.org/10.1016/s0140-6736(79)92765-x.
[7] M. Jang, L. Cai, G.O. Udeani, K.V. Slowing, C.F. Thomas, C.W. Beecher, H.H. Fong, N.R. Farnsworth, A.D. Kinghorn, R.G. Mehta, Cancer Chemopreventive Activity of Resveratrol, a Natural Product Derived from Grapes, Science 275 (1997) 218–220, https://doi.org/10.1126/science.275.5297.218.
[8] S. Rotondo, G. Rajtar, S. Manarini, A. Celardo, D. Rotilio, G. De Gaetano, V. Evangelista, C. Cerletti, Effect of Trans-Resveratrol, a Natural Polyphenolic Compound, on Human Polymorphonuclear Leukocyte Function, Br. J. Pharmacol. 123 (1998) 1691–1699, https://doi.org/10.1038/sj.bjp.0701784.
[9] J.M. López-Nicolás, F. García-Carmona, Aggregation state and pKa values of (E)-resveratrol as determined by fluorescence spectroscopy and UV-visible absorption, J Agric Food Chem. 56 (17) (2008) 7600–7605, https://doi.org/10.1021/jf800843e.
[10] G. Díaz, I.D. Merás, D.A. Rodríguez, Determination of resveratrol in wine by photochemically induced second-derivative fluorescence coupled with liquid-liquid extraction, Anal. Bioanal. Chem. 387 (6) (1999) 1999–2007, https://doi.org/10.1007/s00216-006-1007-z.
[11] K. Robinson, C. Mock, D. Liang, Pre-formulation studies of resveratrol, Drug Dev. Ind. Pharm. 41 (9) (2015) 1464–1469, https://doi.org/10.3109/03639045.2014.958753.
[12] E. Moretón-Lamas, M. Lago-Crespo, M. Lage-Yusty, J. López-Hernández, Comparison of methods for analysis of resveratrol in dietary vegetable supplements, Food Chem. 224 (2017) 219–223, https://doi.org/10.1016/j.foodchem.2016.12.060.

[13] S. Cao, D. Wang, X. Tan, J. Chen, Interaction Between Trans-resveratrol and Serum Albumin in Aqueous Solution, J. Solution Chem. 38 (2009) 1193–1202, https://doi.org/10.1007/s10953-009-9439-7.
[14] X.L. Wei, J.B. Xiao, Y. Wang, Y. Bai, Which model based on fluorescence quenching is suitable to study the interaction between trans-resveratrol and BSA? Spectrochim. Acta A 75 (2009) 299–304, https://doi.org/10.1016/j.saa.2009.10.027.
[15] Novoselov, K.S., Geim, A.K., Morozov, S.V., Jiang, D., Zhang, Y., Dubonos, S.V., Grigorieva, I.V., Firsov, A.A. Electric field effect in atomically thin carbon films, Science 306 (2004) 666–669. https://doi.10.1126/science.1102896.
[16] Díez-Pascual, A.M., Urruela, C.S., Vallés, C., Vera-López, S., San Andrés, M.P. Tailorable Synthesis of Highly Oxidized Graphene Oxides via an Environmentally-Friendly Electrochemical Process, Nanomaterials 10 (2020) 239. https://doi: 10.3390/nano10020239.
[17] S. Vera-López, P. Martínez, M.P. San Andrés, A.M. Díez-Pascual, M. Valiente, Study of graphene dispersions in sodium dodecylsulfate by steady-state fluorescence of pyrene, J. Colloid Int. Sci. 514 (2018) 415–424, https://doi.org/10.1016/j.jcis.2017.12.052.
[18] Mateos, R., Vera-López, S., Valiente, Díez-Pascual, A.M., San Andrés, M.P. Comparison of Anionic, Cationic and Nonionic Surfactants as Dispersing Agents for Graphene Based on the Fluorescence of Riboflavin, Nanomaterials 7 (2017) 403. https://doi:10.3390/nano7110403.
[19] H. Salavagione, A.M. Díez-Pascual, E. Lázaro, S. Vera, M. Gomez-Fatou, Chemical sensors based on polymer composites with carbon nanotubes and grapheme: The role of the polymer, J. Mater. Chem. 2 (2014) 14289–14328, https://doi.org/10.1039/C4TA02159B.
[20] A.C. Mendes Hacke, D. Lima, S. Kuss, Green synthesis of electroactive nanomaterials by using plant-derived natural products, J. Electroanalyt. Chem. 922 (2022), 116786, https://doi.org/10.1016/j.jelechem.2022.116786.
[21] San Andrés, M.P., Baños-Cabrera, M., Gutiérrez-Fernández, L., Díez-Pascual, A.M., Vera-López, S. Fluorescence Study of Riboflavin Interactions with Graphene Dispersed in Bioactive Tannic Acid, Int. J. Mol. Sci. 22 (2021) 5270. https://doi.org/10.3390/ijms22105270.
[22] C. Sainz-Urruela, S. Vera-López, A.M. Díez-Pascual, M.P. San Andrés, Fluorescence study of the influence of centrifugation on graphene oxide dispersions in water and in tannic acid, Spectrochim, Acta A 278 (2022), 121302, https://doi.org/10.1016/j.saa.2022.121302.
[23] F. Silveri, F. Della Pelle, D. Rojas, Q.U. Ain Bukhari, G. Ferraro, E. Fratini, D. Compagnone, (+)-Catechin-assisted graphene production by sonochemical exfoliation in water. A new redox-active nanomaterial for electromediated sensing, Microchim. Acta 188 (2021) 369, https://doi.org/10.1007/s00604-021-05018-2.
[24] F. Silveri, F. Della Pelle, A. Scroccarello, Q.U. Ain Bukhari, M. Del Carlo, D. Compagnone, Modular graphene mediator film-based electrochemical pocket device for chlorpyrifos determination, Talanta 240 (2022), 123212, https://doi.org/10.1016/j.talanta.2022.123212.
[25] S. Manchala, V.S.R.K. Tandava, D. Jampaiah, S.K. Bhargava, V. Shanker, Novel and Highly Efficient Strategy for the Green Synthesis of Soluble Graphene by Aqueous Polyphenol Extracts of Eucalyptus Bark and Its Applications in High-Performance Supercapacitors, ACS Sustainable Chem. Eng. 7 (2019) 11612–11620, https://doi.org/10.1021/acssuschemeng.9b01506.
[26] L. Liu, Y. Zhou, Y. Kang, H. Huang, C. Li, M. Xu, B. Ye, Electrochemical Evaluation of trans-Resveratrol Levels in Red Wine Based on the Interaction between Resveratrol and Graphene, J. Anal. Methods Chem. 2017 (2017) 5749025, https://doi.org/10.1155/2017/5749025.
[27] M.P. San Andrés, A.M. Díez-Pascual, S. Palencia, J. San Torcuato, M. Valiente, S. Vera, Fluorescence quenching of α-tocopherol by graphene dispersed in aqueous surfactant solutions, J. Lumin. 187 (2017) 169–180, https://doi.org/10.1016/j.jlumin.2017.02.056.
[28] K.R. Paton, J. Coleman, Relating the optical absorption coefficient of nanosheet dispersions to the intrinsic monolayer absorption, Carbon 107 (2016) 733–738, https://doi.org/10.1016/j.carbon.2016.06.043.
[29] C. Ferrari, J. Robertson, Interpretation of Raman spectra of disordered and amorphous carbon, Phys. Rev. B 61 (2000) 14095–14107, https://doi.org/10.1103/PhysRevB.61.14095.
[30] F. Tuinstra, J.L. Koenig, Raman Spectrum of Graphite, J. Chem. Phys. 53 (1970) 1126, https://doi.org/10.1063/1.1674108.
[31] Wu, J.; Jiangbin, M.-L.; Tan P.-H. Raman Spectroscopy of Monolayer and Multilayer Graphenes. In book: Raman Spectroscopy of Two-Dimensional Materials, Springer, 2019, pp.1-27.
[32] A. Das, B. Chakraborty, A.K. Sood, Raman Spectroscopy of graphene on different substrates and influence of defects, Bull. Mater. Sci. 31 (2008), 579–584. 10.48550/arXiv.0710.4160.
[33] Zhou, H.; Uysal, A.; Anjos, D.M. Yu Cai, Understanding Defect-Stabilized Noncovalent Functionalization of Graphene, Adv. Mater. Int. 2 (2015) 1500277. 0.1002/admi.201500277.
[34] Zan, R. Microscopy and Spectroscopy of Graphene: Atomic Scale Structure and Interaction with Foreign Atom. Ph.D. Thesis, Manchester University, 2012.
[35] L.J. Cote, J. Kim, V.C. Tung, J. Luo, F. Kim, J. Huang, Graphene oxide as surfactant sheets, Pure Appl. Chem. 83 (2011) 95–110, https://doi.org/10.1351/PAC-CON-10-10-25.
[36] L. Yang, W. Wang, J. Chen, N. Wang, G. Zheng, A comparative study of resveratrol and resveratrol-functional selenium nanoparticles: Inhibiting amyloid β aggregation and reactive oxygen species formation properties. TA coatings on polymeric nanoparticles, J. Biomed. Mater. Res. 106 (2018) 3034–3041, https://doi.org/10.1002/jbm.a.36493.
[37] J.M. López-Nicolás, F. García-Carmona, Aggregation State and pKa Values of (E)-Resveratrol As Determined by Fluorescence Spectroscopy and UV−Visible Absorption, J. Agric. Food Chem. 56 (2008) 7600–7605, https://doi.org/10.1021/jf800843e.